Structure optimizations for excited states with correlated second-order methods: CC2 and ADC(2)

Christof Hättig*

Forschungszentrum Karlsruhe, Institute of Nanotechnology,

P.O. Box 3640, D-76021 Karlsruhe, Germany

Abstract

The performance of the second-order methods for excitation energies CC2 and ADC(2) is investigated and compared with the more approximate CIS and CIS(D) methods as well as with the coupled-cluster models CCSD, CCSDR(3) and CC3. As a by-product of this investigation the first implementation of analytic excited state gradients for ADC(2) and CIS(D_∞) is reported.

It is found that for equilibrium structures and vibrational frequencies the second-order models CIS(D), ADC(2) and CC2 give often results close to those obtained with CCSD. The main advantage of CCSD lies in its robustness with respect to strong correlation effects. For adiabatic excitation energies CC2 is found to give from all second-order methods for excitation energies (inclusive CCSD) the smallest mean absolute errors. ADC(2) and CIS(D_∞) are found to give almost identical results.

An advantage of ADC(2) compared to CC2 is that the excitation energies are obtained as eigenvalues of a Hermitian secular matrix, while in coupled-cluster response the excitation energies are obtained as eigenvalues of a non-Hermitian Jacobi matrix. It is shown that, as a consequence of the lack of Hermitian symmetry, the latter methods will in general not give a physically correct description of conical intersections between states of the same symmetry. This problem does not appear in ADC(2).

*Email: christof.haettig@int.fzk.de

Contents

1 Introduction **2**

2 Relation between CC2, CIS(D_∞) and ADC(2) **5**

3 Intersections of excited states in CC response theory **7**

4 Implementation of analytic excited state gradients for the second-order models ADC(2) and CIS(D_∞) **11**
4.1 The relaxed excited state Lagrange function 11
4.2 The effective one- and two-particle density matrices 13

5 Performance of correlated second-order methods for excited state structures and vibrational frequencies **18**
5.1 Benchmark study on diatomic molecules 20
5.2 Comparison of ADC(2) and CC2 for polyatomic molecules . . 24

6 Summary and Conclusions **30**

A Appendix **34**

1 Introduction

Since the early days of response theory [1, 2, 3, 4] the description of electronic excitations, including ionization and electron attachment, has been a central subject of this branch of theoretical chemistry. Its main idea, the direct calculation of molecular properties as e.g. excitation and ionization energies, transition strengths, frequency-dependent properties, etc. provides a viable alternative to state specific approaches. For frequency-dependent properties the response function approach, i.e. the evaluation of (higher-order) polarization propagators, is today the most successful and efficient route to calculate such quantities. For excitation and ionization energies it bypasses through the evaluation of these quantities as poles of the polarization propagator some subtle balance problems encountered in state specific approaches. But at least as important for the response function or propagator approach to molecular properties has been that it offers a route for the description of electronic excitations with single reference wavefunction models since it does

not require (non-linear) optimizations for excited states. This ansatz is the basis for such successful and widely applied approaches as time-dependent density functional theory (TDDFT) and coupled-cluster response theory.

Partially because of the success of the latter two methods and their availability in several quantum chemistry packages, the interest in earlier ansätze for approximate calculations of polarization propagators or response functions as e.g. the polarization propagator approaches (SOPPA [5, 6, 7], TOPPA [5], etc.) or the algebraic diagrammatic construction [8, 9, 10] has in recent years been relatively limited. These approaches aimed at a direct expansion of the response functions in orders of the electron fluctuation potential without reference to a specific wavefunction model for the ground state. Giving up the reference to a certain model for the ground state energy, introduces additional freedom which allows e.g. to enforce some properties of the exact response function, which else are often lost. On the other hand, if total energies are needed—for example for the determination of equilibrium structures of excited or ionized states—the reference to a specific model for the ground-state energy or wavefunction is unavoidable.

Excitation energies may be taken as an example to demonstrate what is meant above: Given a ground-state model for the energy, a general approach to derive the expressions for the response functions is through the construction of a time-dependent quasi-energy Lagrangian. The latter is made up of the expectation value for the energy $\langle H \rangle$ and some constraints $f_k[H]$ for the (wavefunction) parameters λ_k, both generalized for the time-dependent case by replacing the time-independent Hamiltonian with the Schrödinger operator $H(t) - i\frac{\partial}{\partial t}$:

$$L(\bar{\lambda}_k, \lambda_k, t) = \left\langle H(t) - i\frac{\partial}{\partial t} \right\rangle + \sum_k \bar{\lambda}_k f_k[H(t) - i\tfrac{\partial}{\partial t}](\lambda_{k'}, t) \qquad (1)$$

The expressions for the response functions are then obtained by taking the derivatives of $L(\bar{\lambda}_k, \lambda_k, t)$ with respect to strengths parameters of harmonic time-dependent perturbations with the sum of all frequencies restricted to zero [11, 12, 13]. The poles of the response functions occur at the eigenvalues of the stability matrix of the Lagrangian, i.e. for variational methods (SCF, DFT, MCSCF, CI, etc.) at the eigenvalues of the electronic Hessian

$$\left(\mathbf{E} - \omega_k \mathbf{S}\right) \vec{c}^{\,(k)} = 0 \;, \qquad E_{ij} = \left(\frac{d^2 \langle H \rangle}{d\lambda_i d\lambda_j} \right)_0 \;, \qquad (2)$$

and for non-variational methods, as the coupled-cluster methods are, at the eigenvalues of the electronic Jacobian

$$\Big(\mathbf{A} - \omega_k \mathbf{S}\Big)\vec{c}^{\,(k)} = 0 \;, \qquad\qquad A_{ij} = \left(\frac{d^2 L}{d\bar{\lambda}_i d\lambda_j}\right)_0 \;. \tag{3}$$

For response methods derived from an approximation for the ground-state energy or wavefunction, the expressions for the stability matrix, and thus its structure, properties, and symmetries are determined by the approximations used for the ground-state. In particular, the stability matrix will in general be non-symmetric for any non-variational method. A well-known example for this is the non-symmetric coupled-cluster eigenvalue problem [14, 15]. The loss of Hermitian symmetry leads to different left and right eigenvectors, which increases somewhat the computational costs if both vectors are needed, but else does not give rise to major problems. But a potentially more severe consequence is that eigenvalues may become complex and then can no longer be used to obtain a qualitatively correct and quantitatively accurate description of the corresponding excited states. In propagator type methods which avoid such a connection to a ground-state model these problems can be bypassed by imposing Hermitian symmetry of the stability or secular matrix by construction, as it is done e.g. in SOPPA and in the ADC methods.

In the present article some of the above mentioned problems will be studied at the example of three iterative second-order methods, namely the approximate coupled-cluster singles-and-doubles model [16] CC2, the iterative variant of the doubles correction to configuration interaction singles [17] CIS(D_∞) and the algebraic diagrammatic construction through second order [8, 9] ADC(2). As shown in the next section these three methods are closely related to each other and thus are an interesting example to discuss some aspects of response theory. In Sec. 3 the problems that may arise from non-Hermitian secular matrices will be discussed in connection with conical intersections between two excited states. The remaining sections will be concerned with the implementation of analytic derivatives for CIS(D_∞) and ADC(2), which are a prerequisite for an efficient determination of stationary points on the (excited state) potential energy surfaces, and a comparison of the performance of the three methods CC2, CIS(D_∞) and ADC(2) for equilibrium structures and vibrational frequencies.

2 Relation between CC2 and the CIS(D_∞) and ADC(2) models

For the CC2 model, which has been designed such that for single replacement dominated transitions the excitation energies are correct through second-order in the fluctuation potential, the Jacobian becomes

$$\mathbf{A}^{\mathrm{CC2}} = \left(\begin{array}{c|c} \left\langle {}^{a}_{i}\middle|\left[(\hat{H}+[\hat{H},T_2]),\tau_k^c\right]\middle|\mathrm{HF}\right\rangle & \left\langle {}^{a}_{i}\middle|\left[\hat{H},\tau_{kl}^{cd}\right]\middle|\mathrm{HF}\right\rangle \\ \hline \left\langle {}^{ab}_{ij}\middle|\left[\hat{H},\tau_k^c\right]\middle|\mathrm{HF}\right\rangle & \left\langle {}^{ab}_{ij}\middle|\left[F,\tau_{kl}^{cd}\right]\middle|\mathrm{HF}\right\rangle \end{array}\right) \tag{4}$$

where F is the usual Fock operator and $\hat{H} = \exp(-T_1)H\exp(T_1)$, i.e. a Hamiltonian similarity transformed with the exponential function of the single replacement part of the cluster operator $T = T_1 + T_2$. Here and in the following indices i, j, k, ... are used for orbitals which are occupied in the reference determinant $|\mathrm{HF}\rangle$ and indices a, b, c, ... are used for virtual orbitals. τ_k^c and τ_{kl}^{cd} denote, respectively, single and double replacement operators.

As by-product of its construction as derivative of the residual of ground-state cluster equations, the CC2 Jacobian contains some contributions which would not be needed to obtain excitation energies correct through second-order: the terms introduced via the similarity transformation with $\exp(-T_1)$ contribute only in third and higher orders to the excitation energies of single replacement dominated transitions. The "minimal" Jacobian which gives excitation energies correct through second order is obtained by replacing in $\mathbf{A}^{\mathrm{CC2}}$ the CC2 ground-state cluster amplitudes by the amplitudes from first-order perturbation theory—which implies that the singles replacement part of the cluster operator T_1 vanishes, if the Brillouin condition is fulfilled. The resulting Jacobian is that of the CIS(D_∞) model, an iterative variant of CIS(D) introduced by Head-Gordon et al. [18]:

$$\mathbf{A}^{\mathrm{CIS}(\mathrm{D}_\infty)} = \left(\begin{array}{c|c} \left\langle {}^{a}_{i}\middle|\left[(H+[H,T_2^{(1)}]),\tau_k^c\right]\middle|\mathrm{HF}\right\rangle & \left\langle {}^{a}_{i}\middle|\left[H,\tau_{kl}^{cd}\right]\middle|\mathrm{HF}\right\rangle \\ \hline \left\langle {}^{ab}_{ij}\middle|\left[H,\tau_k^c\right]\middle|\mathrm{HF}\right\rangle & \left\langle {}^{ab}_{ij}\middle|\left[F,\tau_{kl}^{cd}\right]\middle|\mathrm{HF}\right\rangle \end{array}\right) \tag{5}$$

Similar as the CIS(D) perturbative second-order correction to CIS excitation energies, also the CIS(D_∞) excitation energies cannot directly be derived from the response function of a known (ground-state) wavefunction model. A characteristic it has in common with propagator methods. Indeed, the secular matrix for CIS(D_∞) differs only in a small (but important) detail from a propagator method proposed about two decades ago by Schirmer [8]: the algebraic diagrammatic construction through second order ADC(2). The secular matrix used in ADC(2) is just the symmetric or, in the complex case, the Hermitian part of that for the CIS(D_∞) model:

$$\mathbf{A}^{\mathrm{ADC(2)}} = \frac{1}{2}\Big(\mathbf{A}^{\mathrm{CIS(D_\infty)}} + (\mathbf{A}^{\mathrm{CIS(D_\infty)}})^\dagger\Big) \tag{6}$$

Provided that the Hartree-Fock reference determinant fulfills the Brillouin condition $\langle {}^a_i|H|\mathrm{HF}\rangle = 0$, i.e. for a closed-shell or an unrestricted open-shell case, the CIS(D_∞) Jacobian can be rewritten as:

$$\mathbf{A}^{\mathrm{CIS(D_\infty)}} = \left(\begin{array}{c|c} \left\langle {}^a_i\middle|H - E_{\mathrm{HF}}\middle|{}^c_k\right\rangle + \left\langle {}^a_i\middle|\left[[H,T_2^{(1)}],\tau_k^c\right]\middle|\mathrm{HF}\right\rangle & \left\langle {}^a_i\middle|H\middle|{}^{cd}_{kl}\right\rangle \\ \hline \left\langle {}^{ab}_{ij}\middle|H\middle|{}^c_k\right\rangle & \left\langle {}^{ab}_{ij}\middle|F - E_0\middle|{}^{cd}_{kl}\right\rangle \end{array}\right) \tag{7}$$

with $E_{\mathrm{HF}} = \langle \mathrm{HF}|\mathrm{H}|\mathrm{HF}\rangle$ and $E_0 = \langle \mathrm{HF}|\mathrm{F}|\mathrm{HF}\rangle$. Thus, in these cases the symmetrization in Eq. (6) affects only the second-order contribution to the singles-singles block, i.e. the terms proportional to the ground-state doubles $T_2^{(1)}$. All other contributions are already Hermitian.

The above relations between CC2, CIS(D_∞), and ADC(2) provide a simple recipe to implement the latter two methods in an existing CC2 program:

- For CIS(D_∞) the only modification required is that the converged CC2 ground-state amplitudes are replaced by those from first-order perturbation theory.
- For ADC(2) in addition the contributions of $[H, T_2^{(1)}]$ to the singles-singles block have to be symmetrized. This can be achieved with a few additional operations at costs of $\mathcal{O}(n^2N^2)$.

3 Intersections of excited states in coupled-cluster response theory

As pointed out in the introduction, the coupled-cluster response or equation-of-motion methods lead to Jacobi or secular matrices which in general are not symmetric. While this usually does not cause any problems in single-point calculations for vertical excitation spectra or in the optimization of excited state equilibrium structures, it has serious consequences for the topology of the potential surfaces at intersections between excited states.

If one assumes that the Jacobi matrix has been block diagonalized by applying a (non-unitary) transformation

$$\widetilde{\mathbf{A}} = \mathbf{LAR} \qquad \text{with} \quad \mathbf{LR} = \mathbf{1} \,, \tag{8}$$

such that for a pair of nearly degenerate states (i, j) one is left with a 2×2-problem which has been decoupled from all other eigenvalues:

$$\widetilde{\mathbf{A}} = \begin{pmatrix} \ddots & 0 & 0 & 0 \\ 0 & A_{ii} & A_{ij} & 0 \\ 0 & A_{ji} & A_{jj} & 0 \\ 0 & 0 & 0 & \ddots \end{pmatrix} \tag{9}$$

The 2×2 block for this effective two-state problem can in general be written in the form

$$\widetilde{\mathbf{A}}^{2\times 2} = \begin{pmatrix} \bar{E} - \Delta & S - A \\ S + A & \bar{E} + \Delta \end{pmatrix} \tag{10}$$

which gives the eigenvalues $E_{1,2} = \bar{E} \pm \sqrt{\Delta^2 + S^2 - A^2}$. For a symmetric matrix, i.e. when $A = 0$ for all values of the coordinates, the two states will be degenerate if both parameters Δ and S become zero. This leads to the well-known result [19, 20] that (ignoring spin-orbit effects) states of the same symmetry may have a seam of intersection with the dimension $N^{int} - 2$, where N^{int} is the number of internal degrees of freedom (nuclear coordinates). For states of different symmetry S vanishes for symmetry reasons and the intersection seam may have the dimension $N^{int} - 1$.

For a non-symmetric Jacobi matrix, as in general obtained for the iterative coupled-cluster response or equation-of-motion coupled-cluster methods, a number of different cases can be distinguished, depending on the magnitude of the antisymmetric contribution to the coupling A:

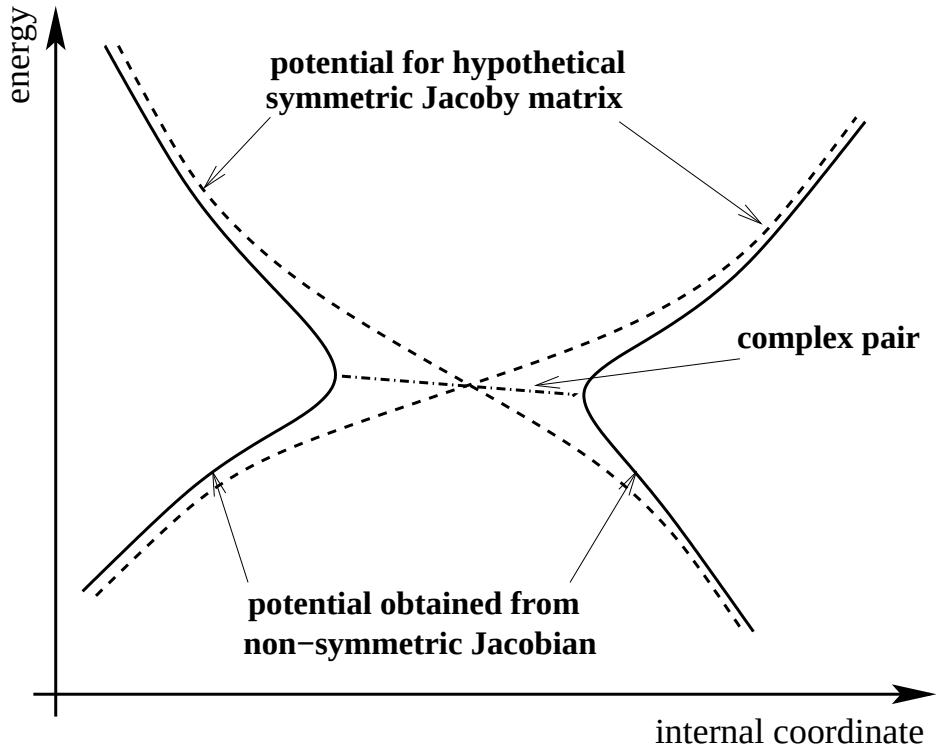


Figure 1: Intersection of two states of the same symmetry as described by a symmetric and a non-symmetric secular matrix. The potential curves obtained with a symmetric secular matrix are shown as broken lines. The full lines are the potential curves for a non-symmetric secular matrix in the region where both eigenvalues are real, while for the region where the eigenvalues are complex only the real part is shown as a dashed and dotted line.

1. $A^2 < \Delta^2 + S^2$, which is the situation usually encountered in single-point calculations for vertical excitation energies and in the optimization of equilibrium structures for excited states: One obtains two real eigenvalues $E_{1,2} = \bar{E} \pm \sqrt{\Delta^2 + S^2 - A^2}$.

2. $A^2 < \Delta^2 + S^2$: this leads to a conjugated pair of degenerate roots with eigenvalues $E_{1,2} = \bar{E} \pm i\sqrt{A^2 - \Delta^2 - S^2}$.

3. $A^2 = \Delta^2 + S^2$, a condition, which for states of the same symmetry in general will be fulfilled in $N^{int} - 1$ dimensions. In this case one obtains an unphysical apparent degeneracy. It can be considered as a kind of instability along a path which connects the two previous cases.

4. only for $A = \Delta = S = 0$ a true intersection of the states is found. For states of the same symmetry this condition will only be fulfilled in $N^{int} - 3$ dimension, i.e. in a manifold which compared to the intersection seam of a symmetric matrix is reduced by one dimension.

Methods with a non-symmetric secular matrix will thus in general not be able to describe conical intersections between states of the same symmetry qualitatively correct. Figure 1 shows a typical two-dimensional cut through potential energy surfaces in a plane where the two states intersect. While a symmetric secular matrix leads to a conical intersection, the potential energy curves obtained with a non-symmetric secular matrix pass—as the intersection is approached—through a point with an (apparent) degeneracy of the two states before a region is entered in which the eigenvalues are complex. This region encloses the intersection seam obtained with a symmetric matrix. At the points with apparent degeneracies the derivatives of the potential energy curves with respect to the coordinate Q become singular.

Figure 2 shows a three-dimensional plot of a similar situation, but now the energy axis has been skipped and instead the points where the two eigenvalues are degenerate are shown in a space spanned by the tuning coordinates of the conical intersection and one coordinate along the intersection seam. In this subspace, the points at which the two states become degenerate with a non-symmetric Jacobian ($A^2 = \Delta^2 + S^2$) form a tube or cone around the intersection seam obtained with a symmetric secular matrix. If the antisymmetric contribution to the off-diagonal matrix element A is a parameter independent of the symmetric contribution S, a true intersection of the two states is only found in a subspace with a dimensionality which—compared

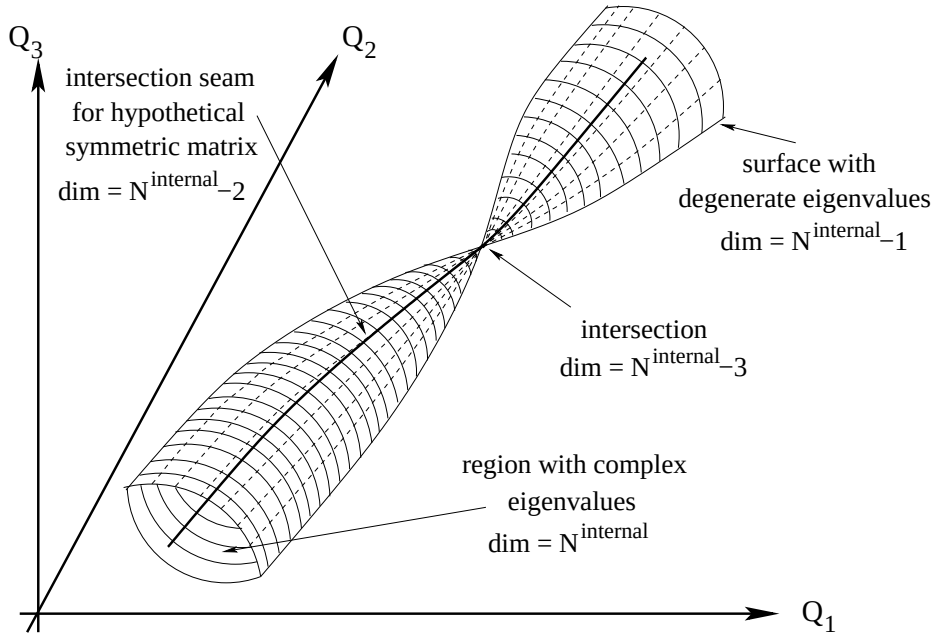


Figure 2: Intersection of two states shown in a space spanned by the two tuning coordinates of the conical intersection and one coordinate along the intersection seam. The thick line is the intersection seam obtained with a symmetric secular matrix. For the non-symmetric matrix the surface on which the two eigenvalues are degenerate is plotted.

to the dimensionality of intersection seam obtained with a symmetric secular matrix—is reduced by one.

The standard coupled-cluster response and equation-of-motion coupled-cluster methods (CC2, CCSD, ...) will thus in general not give a qualitatively correct description of potential energies surfaces (for excited states) at or close to conical intersections. Only if, e.g. because of symmetry reasons, the antisymmetric and the symmetric contribution to the coupling matrix element vanish simultaneously a true intersection will be found. To obtain a qualitatively correct description of intersections between states of the same symmetry requires a symmetric secular matrix. For such problems the algebraic diagrammatic construction methods could be a useful alternative. But in order to make them applicable to intersections in molecules with more than a few atoms, efficient techniques for the localization of stationary points on (excited state) potential energy surfaces are needed [19]. Analytic gradients for excitation energies and total energies of excited states are one important prerequisite for this.

4 Implementation of analytic excited state gradients for ADC(2) and CIS(D_∞)

4.1 The relaxed excited state Lagrange function

Since in contrast to the CC2 model, ADC(2) and CIS(D_∞) are not derived from the response function of a ground state method, there is no unique definition of total energies. One could combine the excitation energies provided by these methods with ground state energies of any suitable method. However, both for consistency to which order in the fluctuation potential correlation effects are accounted for and for computational convenience second-order Møller-Plesset perturbation theory appears to be the most natural choice. With this definition of the total energies, the implementation of analytic gradients for excited states becomes a relatively simple task. Indeed, all the expressions can be obtained as simplifications of those for the CC2 model [21]. In particular, we can define a variational Lagrange function for the total energy of an excited state f as [21, 11, 22]:

$$L^f = \langle \mathrm{HF}|H + [H, T_2]|\mathrm{HF}\rangle + \sum_{i,j=1}^{2} \sum_{\mu_i \nu_j} \bar{E}^f_{\mu_i} A_{\mu_i \nu_j} E^f_{\nu_j} \qquad (11)$$

$$+\omega^f(1-\sum_{i=1}^{2}\sum_{\mu_i}\bar{E}^f_{\mu_i}E^f_{\mu_i})+\bar{t}^f_{\mu_2}\Omega_{\mu_2}+\sum_{\mu_0}\bar{\kappa}^f_{\mu_0}F_{\mu_0}.$$

The first term on the right hand side gives the MP2 ground state energy, with $|\mathrm{HF}\rangle$ the Hartree-Fock reference wave functions and $T_2=\sum_{\mu_2}t_{\mu_2}\tau_{\mu_2}$ the cluster operator for the first-order doubles. (In the following μ_1 or ν_1 will be used to enumerate single replacements and μ_2 or ν_2 for double replacements.)

The second term in Eq. (11) represents the excitation energy and the subsequent term ensures the (bi-)orthonormality of the eigenvectors $\bar{E}^f$ and E^f. To cover both the ADC(2) and the CIS(D_∞) model, we allowed for different left ($\bar{E}^f$) and right (E^f) eigenvectors. Requiring stationarity of the Lagrangian with respect to E^f and $\bar{E}^f$ leads to the left and right eigenvalue problems for the Jacobian $\mathbf{A}$, which determine $\bar{E}^f$, E^f and ω^f. Since for ADC(2) the Jacobian $\mathbf{A}$ is Hermitian, for this model left and right eigenvectors will always be identical.

The last two terms of the Lagrangian in Eq. (11) resemble terms in the Lagrange function for the MP2 ground state energy. The first one determines the Lagrange multipliers $\bar{t}_{\mu_2}$ for the ground states doubles equations,

$$\Omega_{\mu_2}=\langle\mu_2|H+[F,T_2]|\mathrm{HF}\rangle=0 \tag{12}$$

where F is the Fock operator (for the definition of the projection manifold $\langle\mu_2|$ see e.g. Ref. [23]), and the other determines the Lagrange multipliers $\bar{\kappa}_{\mu_0}$ for the Hartree-Fock equations, i.e. it implements the constraint that the subspace μ_0 of the Fock matrix elements is zero. Depending on the choice for the manifold μ_0 one obtains either the Brillouin condition ($F_{ia}=0$) or the canonical condition (diagonal Fock matrix) or an intermediate semi-canonical condition. The Hartree-Fock state is for the following parameterized as

$$|\mathrm{HF}\rangle=\sum_{\mu_0}\exp\left(\kappa_{\mu_0}(\tau_{\mu_0}-\tau^\dagger_{\mu_0})\right)|\mathrm{HF}_0\rangle \tag{13}$$

where $|\mathrm{HF}_0\rangle$ is either the unperturbed state, or if the orbital basis depends on the perturbation—as it does in the case of geometric derivatives and also for magnetic fields if GIAOs are used—a determinant build from the orthonormalized molecular orbital (OMO) basis for the distorted system [24].

Similar as MP2 and CC2, also the ADC(2) and CIS(D_∞) models can be implemented very efficiently using the resolution-of-the-identity (RI) approximation which allows for a fast AO to MO transformation

$$B^Q_{ai}=\sum_P\Big(\sum_\alpha C_{\alpha a}\sum_\beta C_{\beta i}(\alpha\beta|P)\Big)V^{-1/2}_{PQ} \tag{14}$$

and a subsequent fast formation of four-index integrals in the MO basis

$$(ai|bj) \approx (ai|bj)^{\mathrm{RI}} = \sum_{Q} B_{ai}^{Q} B_{bj}^{Q}. \tag{15}$$

In the latter equations $V_{PQ} = (P|Q)$ and $(\alpha\beta|P)$ are, respectively, two- and three-index electron repulsion integrals (ERIs) and P, Q denote orbitals from an auxiliary basis used to resolve the identity. Since only N^3-scaling intermediates are needed on disk, the I/O requirements are reduced drastically compared to a conventional four-index transformation. For further details about the RI approximation, e.g. the choice of auxiliary basis sets and the accuracies obtained for ground and excited state energies and properties, the reader is referred to Refs. [21, 25, 26].

4.2 The effective orbital-relaxed one- and two-particle density matrices

In the present implementation the Hartree-Fock equations are still solved using conventional four-index integrals. Therefore, we need to distinguish between contributions to the Lagrangian which arise from the reference state and the Fock operator and those which are calculated using the RI approximation. However, this is anyway advantageous since it leads to simple expressions to account for a frozen core approximation. For this purpose, we rewrite the Lagrange function, Eq. (11), as

$$\begin{aligned} L &= \langle \mathrm{HF}|H|\mathrm{HF}\rangle + \sum_{\mu_0} \bar{\kappa}_{\mu_0} F_{\mu_0} + \sum_{pq} \Big(D_{pq}^{F,\xi}(\bar{t}) + D_{pq}^{F,A}(\bar{E}, E) \Big) F_{pq} \\ &\quad + \bar{\omega}(1 - \sum_{i=1,2} \sum_{\mu} \bar{E}_{\mu} E_{\mu}) + \frac{1}{2} \sum_{pqrs} \Big(d_{pqrs}^{nsep,\xi}(\bar{t}) + d_{pqrs}^{nsep,A}(\bar{E}, E) \Big) (pq|rs)^{\mathrm{RI}}, \end{aligned} \tag{16}$$

where the superscript f is from now on omitted for brevity. Above, the one-particle densities

$$D_{pq}^{F,\xi}(\bar{t}) = \sum_{\mu_2} \bar{t}_{\mu_2} \langle \mu_2 | [E_{pq}, T_2] | \mathrm{HF} \rangle \tag{17}$$

and

$$\begin{aligned} D_{pq}^{F,A}(\bar{E}, E) &= \sum_{i=1,2} \sum_{\mu_1 \nu_i} \bar{E}_{\mu_1} \langle \mu_1 | [E_{pq}, \tau_{\nu_i}] | \mathrm{HF} \rangle E_{\nu_i} \\ &\quad + \sum_{\mu_2 \nu_2} \bar{E}_{\mu_2} \langle \mu_2 | [E_{pq}, \tau_{\nu_2}] | \mathrm{HF} \rangle E_{\nu_2}. \end{aligned} \tag{18}$$

Table 1: Explicit expressions for the one-particle densities $D^{F,\xi}(\bar{t})$ and $D^{F,A}(\bar{E},E)$ defined in Eqs. (17) and (18).

	$D^{F,\xi}(\bar{t})$	$D^{F,A}(\bar{E},E)$
D_{ij}	$-\sum_{abk}\bar{t}^{ab}_{jk}t^{ab}_{ik}$	$-\sum_{a}\bar{E}_{aj}E_{ai}-\sum_{abk}\bar{E}^{ab}_{jk}E^{ab}_{ik}$
D_{ia}	0	$\sum_{jb}\bar{E}_{bj}(2E^{ab}_{ij}-E^{ba}_{ij})$
D_{ab}	$\sum_{ijc}\bar{t}^{ac}_{ij}t^{bc}_{ij}$	$\sum_{i}\bar{E}_{ai}E_{bi}+\sum_{ijc}\bar{E}^{ac}_{ij}E^{bc}_{ij}$

have been introduced. These densities contain only contributions from the correlation and excitation treatment. The two contributions to the non-separable two-electron density read:

$$d^{nsep,\xi}_{pqrs}(\bar{t}) = \langle \mathrm{HF}|[e_{pqrs},T_2]|\mathrm{HF}\rangle + \sum_{\mu_2}\bar{t}_{\mu_2}\langle\mu_2|e_{pqrs}|\mathrm{HF}\rangle \tag{19}$$

and

$$\begin{aligned} d^{nsep,A}_{pqrs}(\bar{E},E) &= \sum_{\mu_1\nu_1}\bar{E}_{\mu_1}\langle\mu_1|[e_{pqrs},\tau_{\nu_1}]+[[e_{pqrs},\tau_{\nu_1}],T_2]|\mathrm{HF}\rangle E_{\nu_1} \\ &+\sum_{\mu_1\nu_2}\bar{E}_{\mu_1}\langle\mu_1|[e_{pqrs},\tau_{\nu_2}]|\mathrm{HF}\rangle E_{\nu_2}+\sum_{\mu_2\nu_1}\bar{E}_{\mu_2}\langle\mu_2|[e_{pqrs},\tau_{\nu_1}]|\mathrm{HF}\rangle E_{\nu_1}. \end{aligned} \tag{20}$$

Explicit expressions for the densities are given in Tables 1 and 2 for a closed-shell RHF reference determinant and an excited singlet state. For the modifications needed for excited triplet states or for an UHF reference determinant see Refs. [27, 21]. Note that the elements of D^F and d^{nsep} are non-zero only if all indices refer to active orbitals. $D^{F,\xi}_{pq}$ and $d^{nsep,\xi}$ are related to the unrelaxed correlation contributions to the MP2 one- and two-electron densities, which are recovered as $D^{F,\xi}_{pq}(\bar{t}^{\mathrm{MP1}})$ and $d^{nsep,\xi}_{pqrs}(\bar{t}^{\mathrm{MP1}})$ where $\bar{t}^{\mathrm{MP1}}$ are the Lagrangian multipliers from first-order Møller-Plesset perturbation theory. $D^{F,A}$ and $d^{nsep,A}$ contain the contributions from the eigenvectors, which do not have counterparts in the expressions for the MP2 ground state densities.

The equations determining the Lagrangian multipliers $\bar{t}_{\nu_2}$ for the ground state doubles equations are obtained as

$$\sum_{\mu_2}\bar{t}_{\mu_2}\langle\mu_2|[F,\tau_{\nu_2}]|\mathrm{HF}\rangle = -\langle\mathrm{HF}|[H,\tau_{\nu_2}]|\mathrm{HF}\rangle \tag{21}$$

$$- \sum_{\mu_1 \gamma_1} \bar{E}_{\mu_1} \langle \mu_1 | [[H, \tau_{\gamma_1}], \tau_{\nu_2}] | \mathrm{HF} \rangle E_{\gamma_1} \quad .$$

They reduce to the calculation of MP1-like doubles amplitudes with modified two-electron integrals [26, 28, 29] and can in the canonical orbital basis directly be inverted. Similar the double replacement parts of the eigenvectors E and $\bar{E}$ are obtained as:

$$\sum_{\nu_2} \Big(\langle \mu_2 | [F, \tau_{\nu_2}] | \mathrm{HF} \rangle - \omega \delta_{\mu_2 \nu_2} \Big) E_{\nu_2} \quad = \quad - \sum_{\nu_1} \langle \mu_2 | [H, \tau_{\nu_1}] | \mathrm{HF} \rangle E_{\nu_1} \quad , \quad (22)$$

and

$$\sum_{\mu_2} \bar{E}_{\mu_2} \Big(\langle \mu_2 | [F, \tau_{\nu_2}] | \mathrm{HF} \rangle - \omega \delta_{\mu_2 \nu_2} \Big) \quad = \quad - \sum_{\mu_1} \bar{E}_{\mu_1} \langle \mu_1 | [H, \tau_{\nu_2}] | \mathrm{HF} \rangle \quad . \quad (23)$$

The Lagrangian multipliers for the Hartree-Fock equations $\bar{\kappa}$ are determined as usual from a set of CPHF or Z-vector equations:

$$\sum_{AI} \bar{\kappa}_{AI} (A_{AIBJ} - \delta_{AB} \epsilon_A - \delta_{IJ} \epsilon_I) = - \eta^{\kappa}_{BJ} \quad (24)$$

where the indices I, J and A, B denote, respectively, general (i.e. active and frozen) occupied and virtual orbitals and ϵ_p are the SCF orbital energies. The CPHF matrix A_{pqrs} is defined as $A_{pqrs} = 4(pq|rs) - (pr|qs) - (ps|rq)$ with conventional four-index ERIs. The right-hand-side vector for the Z-vector equations can be calculated from the one- and two-particle densities in Eqs. (17)–(20):

$$\begin{aligned} \eta^{\kappa}_{AI} \quad = \quad & \frac{1}{2} \Big(D^{F,ex}_{AI} + D^{F,ex}_{IA} \Big) (\epsilon_I - \epsilon_A) - \frac{1}{4} \sum_{pq} \Big(D^{F,ex}_{pq} + D^{F,ex}_{qp} \Big) A_{pqAI} \quad (25) \\ & + \sum_{prs} \Big[\Big(d^{nsep,ex}_{pArs} + d^{nsep,ex}_{Aprs} \Big) (pI|rs)^{\mathrm{RI}} - \Big(d^{nsep,ex}_{pIrs} + d^{nsep,ex}_{Iprs} \Big) (Ap|rs)^{\mathrm{RI}} \Big], \end{aligned}$$

where for brevity the excited state densities

$$\begin{aligned} D^{F,ex}_{pq} \quad &= \quad D^{F,\xi}_{pq} + D^{F,A}_{pq}, \quad (26) \\ d^{nsep,ex}_{pqrs} \quad &= \quad d^{nsep,\xi}_{pqrs} + d^{nsep,A}_{pqrs}. \quad (27) \end{aligned}$$

were introduced.

Table 2: Explicit expressions for the non-separable two-particle density matrices $d^{F,\xi}(\bar{t})$ and $d^{F,A}(\bar{E},E)$ defined in Eqs. (19) and (20). The intermediate C used for the formulation of $d^{F,A}(\bar{E},E)$ is defined as $C_{ai}=\sum_{jb}\bar{E}_{bj}(2t_{ij}^{ab}-t_{ij}^{ba})$; for the definition of the Lagrangian multipliers $\bar{t}_{ij}^{ab}$ and the symmetrization operator $\mathcal{S}$ see text.

	$d^{\xi}(\bar{t})$	$d^{A}(\bar{E},E)$
d_{ijka}	0	$-\sum_b \bar{E}_{bj}(2E_{ik}^{ba}-E_{ik}^{ab})-\sum_b \bar{E}_{jk}^{ba}E_{bi}$
d_{ijab}	0	$-\bar{E}_{aj}E_{bi}$
d_{iajb}	$4t_{ij}^{ab}-2t_{ij}^{ba}$ $+\bar{t}_{ij}^{ab}$	$\mathcal{S}_{ij}^{ab}\Big\{2C_{ai}E_{bj}-C_{bi}E_{aj}$ $-\sum_k(\sum_c \bar{E}_{ck}E_{cj})(2t_{ki}^{ba}-t_{ki}^{ab})$ $-\sum_c(\sum_k \bar{E}_{ck}E_{bk})(2t_{ji}^{ca}-t_{ji}^{ac})\Big\}$ $+2\bar{E}_{bj}E_{ai}$
d_{iabc}	0	$\sum_j \bar{E}_{bj}(2E_{ij}^{ac}-E_{ij}^{ba})+\sum_j \bar{E}_{ij}^{ab}E_{cj}$

The first derivative of the excited state energy with respect to an external perturbation x can now be evaluated from an expression which is analogous to that for RI-CC2 [28, 21]:

$$\left(\frac{dL}{dx}\right)_{x=0} = \sum_{\alpha\beta} D_{\alpha\beta}^{eff,ao}h_{\alpha\beta}^{[x]}+\frac{1}{2}\sum_{\alpha\beta\gamma\delta} d_{\alpha\beta\gamma\delta}^{sep,ao}(\alpha\beta|\gamma\delta)^{[x]}-\sum_{\alpha\beta} F_{\alpha\beta}^{eff,ao}S_{\alpha\beta}^{[x]} + \sum_{\alpha\beta P}\Delta_{\alpha\beta}^{ao,P}(\alpha\beta|P)^{[x]}-\sum_{PQ}\gamma_{PQ}V_{PQ}^{[x]}, \quad (28)$$

where $h^{[x]}$, $S^{[x]}$, $(\alpha\beta|\gamma\delta)^{[x]}$, $(\alpha\beta|P)^{[x]}$ and $V_{PQ}^{[x]}$ are the derivatives of, respectively, the one-electron Hamiltonian, the overlap and the four-, three- and two-index coulomb integrals in the AO basis and the effective (or relaxed) one-particle density is defined as

$$D_{\alpha\beta}^{eff,ao}=\sum_{pq} C_{\alpha p}C_{\beta q}D_{pq}^{eff}, \quad (29)$$

with

$$D_{pq}^{eff}=D_{pq}^{\mathrm{SCF}}+D_{pq}^{F,\xi}+D_{pq}^{F,A}+\frac{1}{2}(\bar{\kappa}_{pq}+\bar{\kappa}_{qp}). \quad (30)$$

The separable part of the two-electron density is easily constructed on-the-fly during the contraction with the derivatives of the ERIs from D^{eff} and the SCF one-electron density D^{SCF}:

$$d^{sep,ao}_{\alpha\beta\gamma\delta} = \mathcal{S}^{\alpha\beta}_{\gamma\delta}\Big(1 - \frac{1}{2}\mathcal{P}_{\beta\delta}\Big)\Big(D^{eff,ao}_{\alpha\beta} - \frac{1}{2}D^{\mathrm{SCF},ao}_{\alpha\beta}\Big)D^{\mathrm{SCF},ao}_{\gamma\delta} \tag{31}$$

Here, $\mathcal{S}^{\alpha\beta}_{\gamma\delta}$ symmetrizes a function according to $\mathcal{S}^{\alpha\beta}_{\gamma\delta} f^{\alpha\beta}_{\gamma\delta} = f^{\alpha\beta}_{\gamma\delta} + f^{\beta\alpha}_{\delta\gamma}$ and $\mathcal{P}_{\alpha\beta}$ denotes a permutation operator which interchanges two indices.

The non-separable part of the two-electron density is contracted with two- and three-index electron repulsion integrals to the intermediates

$$\Delta^{ao,P}_{\alpha\beta} = \sum_{pq} C_{\alpha p} C_{\beta q} \sum_{rsQ} d^{nsep,ex}_{pqrs} (rs|Q) V^{-1}_{PQ} \tag{32}$$

and

$$\gamma_{PQ} = \sum_{\alpha\beta R} (\alpha\beta|R) \Delta^{ao,P}_{\alpha\beta} V^{-1}_{RQ}. \tag{33}$$

The latter occurs in the gradient expression since also the auxiliary basis depends on the nuclear coordinates which gives rise to a contribution from the first derivative of the metric matrix V_{PQ}. A similar contribution from the overlap matrix of the one-electron basis is contracted with an effective Fock matrix, which can be expressed as

$$\begin{aligned} F^{eff,ao}_{\alpha\beta} &= \frac{1}{2}\sum_{pq} C_{\alpha p} C_{\beta q} \sum_{rst} \Big(d^{nsep,ex}_{rstp} + d^{nsep,ex}_{rspt}\Big)(rs|tq)^{\mathrm{RI}}. \\ &+ \frac{1}{2}\sum_{pq} C_{\alpha p} C_{\beta q}\Big(D^{eff}_{pq} + D^{eff}_{qp}\Big)\epsilon_q + \sum_{Ip} C_{\alpha I} C_{\beta q} \sum_{rs} \Big(D^{F,ex}_{rs} + \bar{\kappa}_{rs}\Big) A_{rsIq} \end{aligned} \tag{34}$$

The implementation of the one- and two-particle density within the framework of the RI approximation and the partitioned doubles-amplitude direct formulation follows closely the algorithms described in Refs. [28] and [21] for the ground and excited state gradients for CC2.

For ADC(2) and CIS(D_∞) the course of a gradient calculation after the solution of the eigenvalue problem (which for CIS(D_∞) implies the determination of both the right and the left eigenvectors) can be be sketched as follows:

- First the eigenvectors are normalized as $\sum_{i=1,2}\sum_{\mu_i} \bar{E}_{\mu_i} E_{\mu_i} = 1$.

- Then the unrelaxed one-electron densities $D^{F,\xi}$ and $D^{F,A}$ and intermediates for the two-electron densities are computed.
- The right-hand-side for the CPHF η^{κ} equations and the effective Fock matrix F^{eff} are set up and the CPHF equations are solved.
- Finally the contributions to the gradient are evaluated by contracting the derivative integrals with the respective densities.

Note, that in contrast to CC2 for ADC(2) and CIS(D_∞) after the solution of the eigenvalue problem no other equations with $\mathcal{O}(N^5)$ scaling costs must be solved iteratively.

5 Performance of correlated second-order methods for excited state structures and vibrational frequencies

From the discussion in Secs. 2 and 3 it follows that for well-isolated states, i.e. far from same-symmetry intersections, the non-Hermitian contribution to the Jacobian in which ADC(2) and CIS(D_∞) differ should have only a small effect on the eigenvalues and vectors. Test calculations on a few diatomic molecules and CH_2O and C_2H_2 show that indeed ADC(2) and CIS(D_∞) give not only vertical excitation energies, but also adiabatic excitation energies, bond lengths and vibrational frequencies, which are almost identical. The differences are close to or fall even below the convergence threshold used for the calculations. Since ADC(2) has both conceptual and computational advantages over CIS(D_∞), the latter model will in the following not be considered further.

In the next two subsections the results of two sets of test calculations are presented. The first test is a comparison of a hierarchy of single-reference methods methods for excited states up to approximated coupled-cluster singles, doubles and triples methods in large basis sets but restricted to diatomic molecules. In the second part only ADC(2) and CC2 are compared for a set of small and medium sized polyatomic molecules for which excited state geometries and frequencies are experimentally well-known.

Table 3: Comparison of ADC(2) and CIS(D_∞) for excitation energies and structures of excited states. The calculations on N_2 and BF where carried out in the aug-cc-pwCVQZ basis sets and all electrons have been active, while for CH_2O and C_2H_2 the aug-cc-pVQZ basis and a frozen core approximation was used. Experimental values taken from Refs. [30, 31, 32].

Molecule	State	Property	CIS(D_∞)	ADC(2)	CC2	Exp.
N_2	$w\ ^1\Delta_u$	T_{vert}	10.629 eV	10.628 eV	10.584 eV	
		T_e	9.36 eV	9.36 eV	9.37 eV	8.94 eV
		R_e	128.1 pm	128.1 pm	129.3 pm	126.8 pm
		ω_e	1449 cm^{-1}	1449 cm^{-1}	1360 cm^{-1}	1559 cm^{-1}
BF	$A\ ^1\Pi$	T_{vert}	6.424 eV	6.424 eV		
		T_e	6.36 eV	6.37 eV	6.36 eV	6.34 eV
		R_e	131.2 pm	131.2 pm	131.4 pm	130.4 pm
		ω_e	1214 cm^{-1}	1214 cm^{-1}	1213 cm^{-1}	1265 cm^{-1}
CH_2O	$1\ ^1A''$	T_{vert}	3.930 eV	3.930 eV	4.025 eV	
		T_0	3.30 eV	3.30 eV	3.52 eV	3.49 eV
		d(CO)	138.2 pm	138.2 pm	135.5 pm	132.3 pm
		ϕ [d]	14.6 deg	14.6 deg	25.7 deg	34.0 deg
		$\nu_2(a')$	1344 cm^{-1}	1344 cm^{-1}	1321 cm^{-1}	1293 cm^{-1}
CH_2O	$1\ ^3A''$	T_{vert}	3.477 eV	3.476 eV	3.556 eV	
		T_0	2.91 eV	2.91 eV	3.05 eV	3.12 eV
		d(CO)	134.5 pm	134.5 pm	133.6 pm	132.3 pm
		ϕ [d]	33.4 deg	33.5 deg	38.1 deg	41.1 deg
		$\nu_2(a')$	1323 cm^{-1}	1320 cm^{-1}	1298 cm^{-1}	1283 cm^{-1}
C_2H_2	$1\ ^1A_u$	T_{vert}	7.224 eV	7.224 eV	7.199 eV	
		T_0		5.38 eV	5.33 eV	5.23 eV
		d(CC)	137.3 pm	137.3 pm	138.1 pm	137.5 pm
		$\nu_2(a_g)$	1426 cm^{-1}	1426 cm^{-1}	1368 cm^{-1}	1385 cm^{-1}

5.1 Benchmark study on the four diatomic molecules N_2, CO, BH, and BF

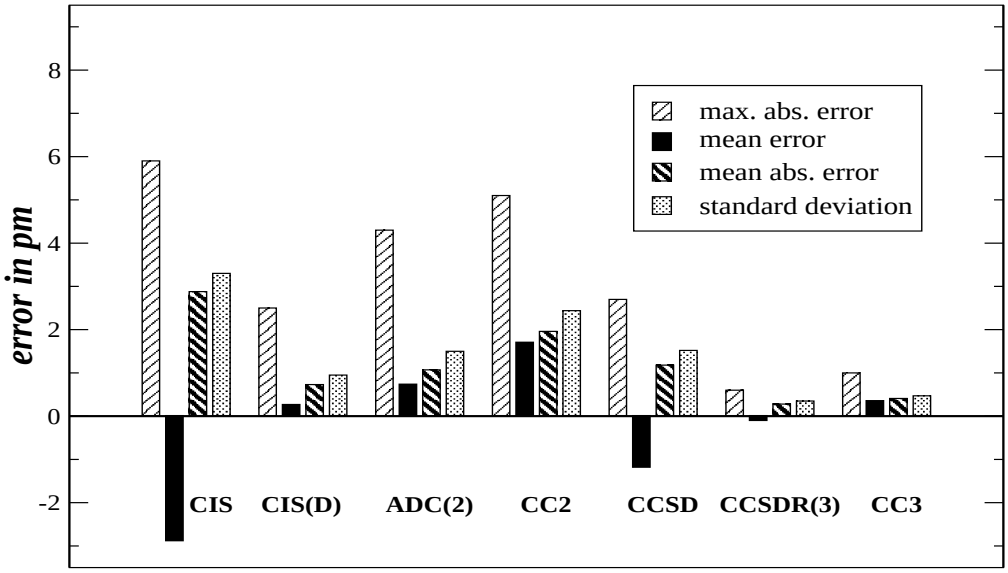


Figure 3: Errors in calculated bond lengths for 19 excited states. Experimental data from Ref. [31]; for technical details of the calculations see text.

For the comparison of the second-order methods for excitation energies with highly correlated methods which account also for the effects of connected triples, four molecules N_2, CO, BH, and BF have been selected since for these several excited states are experimentally well known and have minima at not too far stretched internuclear distances and accurate basis sets are available. The test set consists of 11 singlet and 19 triplet states:

N_2 : $A\ ^3\Sigma_g^+$, $B\ ^3\Pi_g$, $B'\ ^3\Sigma_u^-$, $a'\ ^1\Sigma_u^-$, $a\ ^1\Pi_g$, $w^1\Delta_u$, $C^3\Pi_u$

CO : $a\ ^3\Pi$, $A\ ^1\Pi$, $B\ ^1\Sigma^+$, $C\ ^1\Sigma^+$

BF : $a\ ^3\Pi$, $A\ ^1\Pi$, $B\ ^1\Sigma^+$, $C\ ^1\Sigma^+$, $b\ ^3\Sigma^+$, $d\ ^3\Pi$

BH : $A\ ^1\Pi$, $B\ ^1\Sigma^+$

and the following methods have been included in the comparison:

- configuration interaction singles (CIS), which is equivalent to coupled-cluster singles (CCS)—provided that the Hartree-Fock reference wavefunction fulfills the Brillouin condition
- CIS(D), a perturbative doubles correction to CIS
- the algebraic diagrammatic construction through second order ADC(2)
- the approximate coupled-cluster singles and doubles model CC2
- coupled-cluster singles and doubles (CCSD)
- CCSDR(3), a perturbative triples correction to CCSD—since for this method no implementation for triplet excited states is available, the results for CCSDR(3) include only the 11 singlet states of the test set.
- the approximate coupled-cluster singles, doubles, and triples model CC3

For single excitation dominated transitions, as the investigated states are, CIS is correct through first order in the fluctuation potential, the methods CIS(D), ADC(2), CC2 and CCSD are correct through second order, and CCSDR(3) [33] and CC3 [34, 35] are correct through third order. As in Sec. 4 the total energies for CIS(D) and ADC(2) were defined as the sum of the excitation energies obtained with these models and the MP2 ground state energy, the CCSDR(3) excitation energies were combined with the ground state energies from from the CC(3) perturbative triples correction [33] to CCSD. The CCSD, CCSDR(3), CC(3), and CC3 calculations have been carried out with the Dalton quantum chemistry package [36]; for all other calculations a development version of Turbomole was used.

To avoid any bias of the results due to core correlation effects all electrons have been correlated and the aug-cc-pwCVQZ basis [37, 38, 39, 40] has been used. This basis set should even for the triples methods CCSDR(3) and CC3 give results close to the basis set limit. Detailed results for the bond lengths, the harmonic vibrational frequencies and the adiabatic excitation energies are given in the Appendix. A summary of the results is shown in Fig. $3-5$.

For none of the three investigated quantities (bond lengths, vibrational frequencies and adiabatic excitation energies) the convergence within the coupled-cluster hierarchy is as smooth it is usually found for vertical excitation energies. In particular for the bond lengths and the vibrational

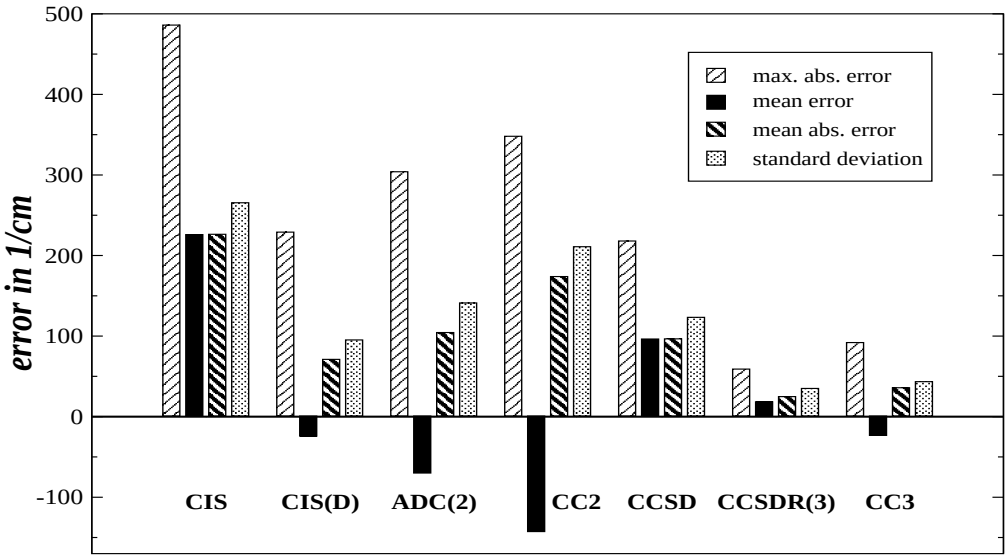


Figure 4: Errors in calculated harmonic frequencies for 19 excited states in N_2, CO, BH, and BF. Experimental reference data taken from Ref. [31]; for technical details of the calculations see text.

frequencies the results indicate some oscillations within the CC model hierarchy, similar to that found for ground state bond length and vibrational frequencies [23]: CIS gives, similar as SCF for the ground state, much too short bond lengths—for the 19 states included in this test set R_e is on the average underestimated by about 3 pm. CC2 overestimates the correlation contribution and thus the bond lengths and their change upon excitation, while CCSD gives again too short bond lengths, even though CCSD is much more robust with respect to strong correlation effects, as encountered in N_2 and CO if the bond is stretched upon excitation from a bounding into an anti-bonding orbital. After inclusion of the effects of connected triples at the CCSDR(3) and the CC3 level the results are very accurate.

Compared to CC2 the ADC(2) model profits from the somewhat better stability of the underlying MP2 for the ground state, while the results for the perturbative doubles correction CIS(D) are intermediate between the results for CIS and ADC(2). However, two of the example molecules, N_2 and CO, are difficult cases for single-reference methods and in particular for CC2. Taking this into accound, one can, based on the above trends, expect that for single

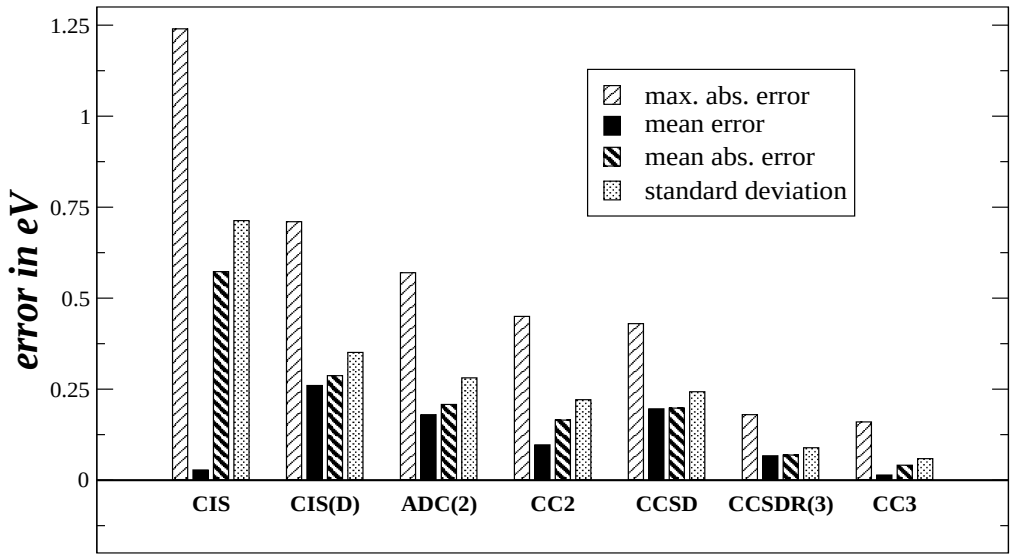


Figure 5: Errors in adiabatic excitation energies for 19 excited states in N_2, CO, BH, and BF. Experimental reference data taken from Ref. [31]; for technical details of the calculations see text.

replacement dominated excited states CC2 and CC3 for larger molecules with polyatomic chromophores give equilibrium geometries of similar accuracy as obtained with these methods for the ground state, i.e. close to the accuracy obtained with, respectively MP2 and CCSD(T). Similar, CCSD cannot be expected to give for excited states geometries which are more accurate than those for ground states. Its main advantage lies in its robustness.

The results for harmonic frequencies corroborate the above observations. For almost all excited states it is found that the vibrational frequencies are overestimated (underestimated) the more the bond lengths are underestimated (overestimated). Thus, CIS and, to a lesser extend, CCSD give too high vibrational frequencies, while CC2 usually yields to low vibrational frequencies. Again, after inclusion of approximate triples in the methods CCSDR(3) and CC3 the results are close to the experimental values.

In contrast to the smooth convergence of vertical excitation energies in the hierarchy CCS – CC2 – CCSD – CC3, the adiabatic excitation energies change more irregular: no improvement is obtained when going from CC2 to CCSD. The CCSD results have about the same accuracy as those obtained

with ADC(2). The results obtained with the perturbative doubles correction CIS(D) are slightly larger. First after the inclusion of connected triples at the CCSDR(3) and CC3 level a systematic and significant improvement upon CC2 is obtained.

5.2 Comparison of ADC(2) and CC2 for polyatomic molecules

The benchmark results from the previous subsection include only states in four diatomic molecules. It will of cause require further studies, in particular for polyatomic molecules to see how general these findings are. But, for polyatomic molecules excitations are usually delocalized over chromophores which comprise several atoms and, as a consequence, the changes in the bond lengths upon excitation will be more moderate than they are in small molecules.

This means that the results will be much more dominated by the performance of the underlying ground state method. Though, one would expect for polyatomic molecules—in particular if the differences between the bond lengths in the ground and the excited states are not large—that the approximate doubles methods ADC(2) and CC2 give results of almost the same accuracy as obtained for ground state geometries with MP2 and CC2. However, for small molecules like CH_2O, C_2H_2, where the excitation process is essentially localized at one bond, similar difficulties as found above for the diatomic molecules have to be expected.

In Tables 4 – 6 some results are listed for 0-0 transition energies, equilibrium bond lengths and angles and vibrational frequencies for 13 excited states of small polyatomic molecules, where accurate experimental results are available. The CC2 results, which have been taken from Ref. [21], and the ADC(2) results, which are from the present work, have been obtained in the aug-cc-pVQZ basis sets (aug-cc-pV(Q+d)Z for the atoms Si–Cl) [37, 38, 39, 42]. The frozen core approximations has been used throughout, with the 1s orbitals frozen for the atoms B–F and 1s2s2p frozen for Si–Cl.

In contrast to the diatomic molecules investigated in Sec. 5.1, where from the experimental data values for T_e, R_e and ω_e could be extracted, for the excited states in these molecules experimental data is only available for T_0, R_0 and fundamental frequencies. This limits somewhat the comparability with the calculated values, which have been obtained within the harmonic

Table 4: 0–0 transition energies (in eV) in the harmonic approximation.

Molecule	State	CC2	ADC(2)	Exp.
SO_2	$1\ ^3B_1$	2.92	2.94	3.19[a]
SiF_2	$1\ ^1B_1$	5.49	5.44	5.34[b]
CCl_2	$1\ ^1B_1$	2.11	2.00	2.14[b]
CS_2	$1\ ^3A_2$	3.29	3.18	3.25[a]
HCN	$1\ ^1A''$	6.72	6.82	6.48[a]
HCP	$1\ ^1A''$	4.48	4.51	4.31[a]
C_2H_2	$1\ ^1A_u$	5.33	5.38	5.23[a]
CH_2O	$1\ ^1A''$	3.52	3.30	3.49[c]
	$1\ ^3A''$	3.05	2.91	3.12[c]
CH_2S	$1\ ^1A_2$	2.15	2.03	2.03[c]
	$1\ ^3A''$	1.79	1.69	1.80[c]
CHOCHO	$1\ ^1A_u$	2.70	2.63	2.72[a]
HC_2CHO	$1\ ^1A''$	3.17	2.90	3.24[a]

[b]From Ref. [31]. [b]From Ref. [41]. [c]From Ref. [32]

approximation. This impairs in particular the results for C-H bond lengths and the corresponding stretchings modes, for which anharmonic effects are sizable.

The results listed in Tables 4 – 6 indicate that the above anticipated trends are indeed found for polyatomic molecules. In the 0-0 transition energies f.ex. the mean absolute error (MAE) is for CC2 0.1 eV, only for SO_2 and HCN the errors are larger than 0.2 eV. Also for ADC(2) the MAE of 0.17 eV for these polyatomic molecules is considerable smaller than for the diatomic molecules studied in Sec. 5.1. Interestingly, the difference in mean absolute errors for CC2 and ADC(2) is almost the same for the excited states in the polyatomic molecules listed in Table 4 and for the excited states in the diatomic molecules (Table 9) studied in the previous subsection.

Table 5: Excited state structure parameters (bond lengths in pm and angles in degrees) calculated with CC2 and ADC(2). Unless otherwise stated the experimental data was taken from Refs. [31, 30].

Molecule	State	Parameter	CC2	ADC(2)	Exp.
SO_2	$1\ ^3B_1$	d(SO)	155.4	151.8	149.4
		$\angle$(OSO)	128.8	126.5	126.1
SiF_2 [a]	$1\ ^1B_1$	d(SiF)	162.8	162.3	160.1
		$\angle$(FSiF)	115.9	116.0	115.9
CCl_2 [a]	$1\ ^1B_1$	d(CCl)	164.8	164.7	165.2
		$\angle$(ClCCl)	132.0	131.6	131.4
CS_2	$1\ ^3A_2$	d(CS)	164.9	163.7	164.0
		$\angle$(SCS)	135.7	136.7	135.8
HCN	$1\ ^1A''$	d(CH)	111.5	111.3	114.0
		d(CN)	132.1	129.3	129.7
		$\angle$(HCN)	122.3	127.6	125.0
HCP	$1\ ^1A''$	d(CP)	171.6	168.2	169.0
		$\angle$(HCP)	128.4	137.1	128.0
C_2H_2 [b]	$1\ ^1A_u$	d(CC)	138.1	137.3	137.5
		d(CH)	109.2	109.1	110.5
		$\angle$(HCC)	122.0	122.2	121.4
CH_2O [c]	$1\ ^1A''$	d(CH)	108.7	108.4	109.8
		d(CO)	135.5	138.2	132.3
		$\angle$(HCH)	121.6	124.1	118.4
		ϕ [d]	25.7	14.6	34.0
CH_2O [c]	$1\ ^3A''$	d(CH)	109.2	108.9	108.4
		d(CO)	133.6	134.5	130.7
		$\angle$(HCH)	118.0	119.8	117.9
		ϕ [d]	38.1	33.5	41.1
CH_2S [c]	$1\ ^1A_2$	d(CH)	108.3	108.3	107.7
		d(CS)	170.6	171.9	168.2
		$\angle$(HCH)	121.2	121.2	120.7

Table 5: (continued)

Molecule	State	Parameter	CC2	ADC(2)	Exp.
CH_2S [c]	$1\ ^3A''$	d(CH)	108.2	108.2	108.2
		d(CS)	168.9	169.3	168.3
		$\angle$(HCH)	120.5	121.3	119.3
		ϕ [d]	15.0	4.3	11.9
trans-$(CHO)_2$ [e]	$1\ ^1A_u$	d(CC)	147.9	147.7	146.0
		d(CH)	109.5	109.4	112.0
		d(CO)	125.4	125.0	125.0
		$\angle$(HCC)	114.5	114.9	114.0
		$\angle$(OCC)	123.9	123.6	124.0
HC_2CHO	$1\ ^1A''$	$d(C_1C_2)$	123.8	122.9	123.8
		$d(C_1H)$	106.3	106.3	107.5
		$d(C_2C_3)$	136.0	135.8	136.4
		$d(C_3H)$	108.5	108.3	109.1
		$d(C_3O)$	140.6	144.9	132.5

[a]Experimental values from [41]. [b]Experimental values from [43]. [c]Experimental values from [32]. [d]Out-of-plane angle of the oxygen or sulfur atom, respectively. [e]Experimental values from Ref. [44].

Table 6: Harmonic vibrational frequencies (cm^{-1}) calculated with CC2 and ADC(2). Unless stated otherwise, the experimental values are taken from Refs. [31, 30].

Molecule	State	Mode	CC2	ADC(2)	Exp.
SO_2	$1\ ^3B_1$	$\nu_1(a_1)$	673	852	906
		$\nu_2(a_1)$	285	337	360
SiF_2	$1\ ^1B_1$	$\nu_1(a_1)$	705	714	598
		$\nu_2(a_1)$	235	236	342
CCl_2 [a]	$1\ ^1B_1$	$\nu_1(a_1)$	641	643	634
		$\nu_2(a_1)$	308	310	303

Table 6: (continued)

Molecule	State	Mode	CC2	ADC(2)	Exp.
CS_2	$1\ ^3A_2$	$\nu_1(a_1)$	682	727	692
		$\nu_2(a_1)$	243	311	311
HCN	$1\ ^1A''$	$\nu_2(a')$	1345	1661	1496
		$\nu_3(a')$	963	973	941
HCP	$1\ ^1A''$	$\nu_2(a')$	888	1061	951
		$\nu_3(a')$	636	647	567
C_2H_2	$1\ ^1A_u$	$\nu_2(a_g)$	1368	1426	1385
		$\nu_3(a_g)$	1086	1088	1048
CH_2O [b]	$1\ ^1A''$	$\nu_1(a')$	3064	3107	2846
		$\nu_2(a')$	1321	1344	1293
		$\nu_3(a')$	1015	859	1183
		$\nu_5(a'')$	3202	3255	2968
		$\nu_6(a'')$	873	867	904
	$1\ ^3A''$	$\nu_2(a')$	1298	1320	1283
CH_2S [b]	$1\ ^1A_2$	$\nu_1(a_1)$	3127	3124	3034
		$\nu_2(a_1)$	1343	1346	1320
		$\nu_3(a_1)$	799	751	859
		$\nu_4(b_1)$	3253	3254	3081
		$\nu_5(b_1)$	769	772	799
		$\nu_2(a')$	1337	1342	1320
		$\nu_3(a')$	846	826	859

Table 6: (continued)

Molecule	State	Mode	CC2	ADC(2)	Exp.
trans-$(CHO)_2$ [c]	$1\ ^1A_u$	$\nu_1(a_g)$	3052	3070	2809
		$\nu_2(a_g)$	1369	1410	1391
		$\nu_3(a_g)$	1233	1252	1195
		$\nu_4(a_g)$	995	1019	952
		$\nu_5(a_g)$	494	504	509
		$\nu_6(a_u)$	754	760	720
		$\nu_7(a_u)$	219	221	233
		$\nu_8(b_g)$	763	782	735
		$\nu_{10}(b_u)$	1248	1219	1281
		$\nu_{11}(b_u)$	1176	1096	1172
		$\nu_{12}(b_u)$	372	372	379
HC_2CHO [d]	$1\ ^1A''$	$\nu_2(a')$	3170	3200	2953
		$\nu_3(a')$	1898	1970	1946
		$\nu_4(a')$	1218	1205	1304
		$\nu_5(a')$	1074	1090	1120
		$\nu_6(a')$	780	695	952
		$\nu_7(a')$	642	655	650
		$\nu_8(a')$	471	477	507
		$\nu_9(a')$	171	172	189
		$\nu_{10}(a'')$	550	593	507
		$\nu_{11}(a'')$	416	449	390
		$\nu_{12}(a'')$	324	340	346

[a]Experimental values from Ref. [41]. [b]Experimental values from Ref. [32].
[c]Experimental values from Ref. [45]. [d]Experimental values from Ref. [46].

For bond lengths and angles and for vibrational frequencies the performance of the two methods is—at least for the present test set—on the average very similar. ADC(2) improves upon CC2 in several cases where multiple bonds are weakend upon excitation, es e.g. for HCN, HCP, C_2H_2 or the difficult case of SO_2. On the other hand, ADC(2) performs inferior for $n \rightarrow \pi^*$ transitions as in CH_2O, CH_2S and HC_2CHO, where it gives by far too long C-O distances and too low frequencies for the modes involving these bonds. However, one has to keep in mind that the calculated CC2 and ADC(2) re-

sults are not strictly comparable to the experimental reference data, since in in the calculations anharmonic effects have been neglected. Even though this is not expected, it cannot, without further investigations, be excluded that corrections from the anharmonicities will change the conclusions about the performance of CC2 and ADC(2) for excited state equilibrium structures.

6 Summary and Conclusions

The coupled-cluster methods CCS (CIS), CIS(D), CC2, CCSD, CCSDR(3), and CC3 form today a relatively well-established hierarchy of black-box methods for excited states. With the implementation of analytic gradients [21, 47, 48, 49] it is for some of these methods now possible to obtain equilibrium structures for electronically excited states of small and medium sized molecules in an almost routine manner.

The benchmark study in Sec. 5.1 which compares the performance these methods indicates, in agreement with previous results in the literature [49, 50, 51, 52], that the accuracies obtained for equilibrium structures and harmonic frequencies of single excitation dominated excited states are almost comparable to those obtained for the ground state. It is found that CCSD, even though much more robust with respect to strong correlation effects than the approximate singles-and-doubles methods CIS(D), ADC(2), and CC2, is in general for equilibrium structures not systematically more accurate than these methods. As a consequence CCSD is also not able to improve for adiabatic excitation energies upon the results obtained at the CC2 level.

A drawback of the standard CC response or equation-of-motion CC methods is the lack of Hermitian symmetry of the Jacobi or secular matrix. While this will usually not affect their performance for equilibrium structures, it leads to qualitative wrong results for the potential energy surfaces of excited states in the vicinity of intersections between states of the same symmetry: instead of a conical intersection seam these methods will give a region with a conjugated pair of complex eigenvalues. Propagator type methods, as the algebraic diagrammatic construction (ADC) models, which have a Hermitian secular matrix could for such situations be a valuable alternative.

In Sec. 4 the equations for orbital-relaxed one- and two-particle densities and analytic gradients of excited states have been derived for the ADC(2) and the CIS(D_∞) model. These have been implemented in the RICC2 module [53] of the Turbomole package [54] and were used to investigate the performance

of ADC(2) for excited state potential energy surfaces. The results presented in Secs. 5.1 and 5.2 show, that ADC(2) gives equilibrium structures and harmonic frequencies with an accuracy comparable to that of CC2. In some cases, as for example N_2 and CO, ADC(2) is due to the underlying MP2 ground state more robust than CC2. Only for excitation energies ADC(2) gives somewhat larger errors than CC2.

Acknowledgments

This work is dedicated to Prof. Jan Linderberg and Prof. Poul Jørgensen on the occasion of their, respectively, 70th and 60th birthdays. I am grateful to Poul Jørgensen for having given me the opportunity to join the Theoretical Chemistry group at the Århus university as a postdoc from 1996–1999. I wish to thank both Poul and Jan for their hospitality during these years and all my later visits in Århus. I am looking forward to many more of them.

I thank Jochen Schirmer and Andreas Köhn for a number of useful discussion about ADC(2) and CC2.

References

[1] D. N. Zubarev, Usp. Fiz. Nauk (English translation Soviet Phys. Uspekhi 3 (1960) 320). **71** (1960).

[2] J. Linderberg and Y. Öhrn, Proc. Roy. Soc. (London) A. **285**, 445 (1965).

[3] Y. Öhrn and J. Linderberg, Phys. Rev. A. **139**, 1063 (1965).

[4] J. Linderberg and Y. Öhrn. *Propagators in Quantum Chemistry.* Academic Press, London, 1973.

[5] J. Oddershede, Adv. Quantum Chem. **11**, 275 (1978).

[6] E. S. Nielsen, P. Jørgensen and J. Oddershede, J. Chem. Phys. **73**, 6238 (1980).

[7] J. Oddershede and E. N. Svendsen, Chem. Phys. **64**, 359 (1982).

[8] J. Schirmer, Phys. Rev. A. **26**, 2395 (1981).

[9] A. B. Trofimov and J. Schirmer, J. Phys. B. **28**, 2299 (1995).

[10] A. B. Trofimov, N. M. Vitkovskaya and J. Schirmer, Zhurnal Fizicheskoi Khimii. **71**, 2197 (1997).

[11] O. Christiansen, P. Jørgensen and C. Hättig, Int. J. Quantum Chem. **68**, 1 (1998).

[12] C. Hättig, O. Christiansen and P. Jørgensen, J. Chem. Phys. **108**, 8331 (1998).

[13] T. B. Pedersen and H. Koch, J. Chem. Phys. **108**, 5194 (1998).

[14] H. Koch, H. J. A. Jensen, P. Jørgensen and T. Helgaker, J. Chem. Phys. **93**, 3345 (1990).

[15] J. F. Stanton and R. J. Bartlett, J. Chem. Phys. **98**, 7029 (1993).

[16] O. Christiansen, H. Koch and P. Jørgensen, Chem. Phys. Lett. **243**, 409 (1995).

[17] M. Head-Gordon, R. J. Rico, M. Oumi and T. J. Lee, Chem. Phys. Lett. **219**, 21 (1994).

[18] M. Head-Gordon, M. Oumi and D. Maurice, Mol. Phys. **96**, 593 (1999).

[19] D. R. Yarkony, J. Phys. Chem. A. **105**, 6277 (2001).

[20] J. von Neumann and E. Wigner, Zeit. f. Phys. **30**, 467 (1929).

[21] A. Köhn and C. Hättig, J. Chem. Phys. **119**, 5021 (2003).

[22] C. Hättig and P. Jørgensen, J. Chem. Phys. **109**, 9219 (1998).

[23] T. Helgaker, P. Jørgensen and J. Olsen. *Molecular Electronic-Structure Theory.* John Wiley & Sons, New York, 2000.

[24] T. Helgaker and P. Jørgensen, Adv. Quant. Chem. **19**, 183 (1988).

[25] F. Weigend, A. Köhn and C. Hättig, J. Chem. Phys. **116**, 3175 (2002).

[26] C. Hättig and A. Köhn, J. Chem. Phys. **117**, 6939 (2002).

[27] C. Hättig and K. Hald, Phys. Chem. Chem. Phys. **4**, 2111 (2002).

[28] C. Hättig, J. Chem. Phys. **118**, 7751 (2003).

[29] C. Hättig, A. Köhn and K. Hald, J. Chem. Phys. **116**, 5401 (2002).

[30] K. P. Huber and G. Herzberg. *Molecular Spectra and Molecular Structure: III. Electronic Spectra and Electronic Structure of Polyatomic Molecules.* Van Nostrand Reinhold, New York, 1966.

[31] K. P. Huber and G. Herzberg. *Molecular Spectra and Molecular Structure: IV. Constants of Diatomic Molecules.* Van Nostrand, New York, 1979.

[32] D. J. Clouthier and D. A. Ramsay, Ann. Rev. Phys. Chem. **34**, 31 (1983).

[33] O. Christiansen, H. Koch and P. Jørgensen, J. Chem. Phys. **105**, 1451 (1996).

[34] H. Koch, O. Christiansen, P. Jørgensen, A. Sánchez de Merás and T. Helgaker, J. Chem. Phys. **106**, 1808 (1997).

[35] O. Christiansen, H. Koch and P. Jørgensen, J. Chem. Phys. **103**, 7429 (1995).

[36] T. Helgaker, H. J. Å. Jensen, P. Jørgensen, J. Olsen, K. Ruud, H. Ågren, A. A. Auer, K. L. Bak, V. Bakken, O. Christiansen, S. Coriani, P. Dahle, E. K. Dalskov, T. Enevoldsen, B. Fernandez, C. Hättig, K. Hald, A. Halkier, H. Heiberg, H. Hettema, D. Jonsson, S. Kirpekar, R. Kobayashi, H. Koch, K. V. Mikkelsen, P. Norman, M. J. Packer, T. B. Pedersen, T. A. Ruden, A. Sanchez, T. Saue, S. P. A. Sauer, B. Schimmelpfennig, K. O. Sylvester-Hvid, P. R.Taylor, and O.Vahtras. Dalton – an electronic structure program, release 1.2, 2001.

[37] T. H. Dunning, J. Chem. Phys. **90**, 1007 (1989).

[38] D. E. Woon and T. H. Dunning, J. Chem. Phys. **98**, 1358 (1993).

[39] D. E. Woon and T. H. Dunning, J. Chem. Phys. **100**, 2975 (1994).

[40] K. A. Peterson and T. H. Dunning, J. Chem. Phys. **117**, 10548 (2002).

[41] D. J. Clouthier and J. Karolczak, J. Chem. Phys. **94**, 1 (1991).

[42] T. H. Dunning, K. A. Peterson and A. K. Wilson, J. Chem. Phys. **114**, 9244 (2001).

[43] T. R. Huet, M. Godefroid and M. Herman, J. Mol. Spectrosc. **114**, 32 (1990).

[44] J. M. Hollas. *Molecular structure from rotational and vibrational transitions in electronic spectra*, in *Recent Experimental and Computational Advances in Molecular Spectroscopy*, edited by R. Fausto, pp. 32–61. Kluwer, Dordrecht, 1993.

[45] R. Y. Dong, R. Nanes and D. A. Ramsay, Can. J. Chem. **71**, 1595 (1993).

[46] J. C. D. Brand, J. H. Calloman and J. K. G. Watson, Discussions of the Faraday Society. **35**, 175 (1963).

[47] J. B. Foresman, M. Head-Gordon, J. A. Pople and M. J. Frisch, J. Phys. Chem. **96**, 135 (1992).

[48] J. F. Stanton, J. Chem. Phys. **99**, 8840 (1993).

[49] J. F. Stanton and J. Gauss, J. Chem. Phys. **100**, 4695 (1994).

[50] J. F. Stanton, J. Gauss, N. Ishikawa and M. Head-Gordon, J. Chem. Phys. **103**, 4160 (1995).

[51] K. W. Sattelmeyer, J. F. Stanton, J. Olsen and J. Gauss, Chem. Phys. Lett. **347**, 499 (2001).

[52] H. Larsen, J. Olsen, P. Jørgensen and O. Christiansen, J. Chem. Phys. **113**, 6077 (2000). Erratum ibid. 114 (2001) 10985.

[53] C. Hättig and F. Weigend, J. Chem. Phys. **113**, 5154 (2000).

[54] R. Ahlrichs, M. Bär, M. Häser, H. Horn and C. Kölmel, Chem. Phys. Lett. **162**, 165 (1989).

A Appendix

In the three tables below the data underlying Figs. 3–5 is collected.

Table 7: Bond lengths R_e (pm) of diatomic molecules. For the technical details see Sec. 5.1; experimental values from Ref. [31].

Molecule	State	CIS	CIS(D)	ADC(2)	CC2	CCSD	CCSDR(3)	CC3	Exp.
N_2	A $^3\Sigma_u^+$	122.8	129.0	129.4	131.5	126.8	-	129.3	128.7
	B $^3\Pi_g$	117.6	122.2	123.1	124.9	119.5	-	121.4	121.3
	B′ $^3\Sigma_u^-$	123.3	128.6	129.2	130.7	125.2	-	128.3	127.8
	a′ $^1\Sigma_u^-$	123.3	128.5	129.0	130.4	124.8	126.9	128.0	127.5
	a $^1\Pi_g$	119.0	123.0	124.5	126.5	120.1	121.5	122.2	122.0
	w $^1\Delta_u$	122.8	127.6	128.1	129.3	124.2	126.3	127.4	126.8
	C $^3\Pi_u$	110.1	114.3	115.4	116.3	113.1	-	114.6	114.9
CO	a $^3\Pi$	117.5	121.0	121.4	122.7	119.4	-	121.1	120.6
	A $^1\Pi$	121.0	126.0	127.8	128.6	122.2	123.3	124.5	123.5
	B $^1\Sigma^+$	108.5	112.3	112.6	113.8	110.9	112.1	112.5	112.0
	C $^1\Sigma^+$	108.2	111.7	112.0	113.5	110.8	112.0	112.4	112.2
BF	a $^3\Pi$	129.8	131.5	131.6	131.9	130.6	-	131.1	130.8
	A $^1\Pi$	128.4	131.1	131.2	131.4	130.1	130.5	130.7	130.4
	b $^3\Sigma^+$	120.0	121.3	121.4	121.9	121.1	-	121.9	121.5
	B $^1\Sigma^+$	119.3	120.4	120.5	121.0	120.2	120.9	121.0	120.7
	C $^1\Sigma^+$	120.8	122.1	122.2	122.7	121.8	122.4	122.5	122.0
	d $^3\Pi$	119.9	121.0	121.0	121.5	120.7	-	121.5	121.0
BH	A $^1\Pi$	120.3	120.6	120.5	120.6	121.9	122.1	122.2	121.9
	B $^1\Sigma^+$	119.9	120.2	120.4	120.5	121.4	121.5	121.5	121.6

Table 8: Harmonic vibrational frequencies ω_e (cm^{-1}) of diatomic molecules. For the technical details see Sec. 5.1; experimental values from Ref. [31].

Molecule	State	CIS	CIS(D)	ADC(2)	CC2	CCSD	CCSDR(3)	CC3	Exp.
N_2	A $^3\Sigma_u^+$	1873	1407	1379	1223	1582	-	1420	1461
	B $^3\Pi_g$	2008	1653	1576	1432	1884	-	1728	1733
	B′ $^3\Sigma_u^-$	1841	1440	1402	1290	1701	-	1480	1517
	a′ $^1\Sigma_u^-$	1841	1447	1412	1303	1732	1582	1491	1530
	a $^1\Pi_g$	1904	1616	1505	1353	1858	1753	1685	1694
	w $^1\Delta_u$	1859	1483	1449	1360	1752	1604	1509	1559
	C $^3\Pi_u$	2533	2133	1994	1885	2265	-	2113	2047
CO	a $^3\Pi$	1965	1686	1645	1542	1830	-	1688	1743
	A $^1\Pi$	1646	1326	1214	1170	1594	1536	1426	1518
	B $^1\Sigma^+$	2480	1982	1830	1815	2233	2120	2064	2113
	C $^1\Sigma^+$	2488	2154	2111	1945	2287	2174	2124	2176
BF	a $^3\Pi$	1379	1298	1291	1277	1334	9999	1314	1324
	A $^1\Pi$	1365	1238	1214	1213	1279	1259	1251	1265
	b $^3\Sigma^+$	1744	1638	1631	1592	1652	9999	1599	1629
	B $^1\Sigma^+$	1784	1711	1699	1666	1724	1689	1670	1694
	C $^1\Sigma^+$	1703	1612	1607	1577	1631	1601	1587	1613
	d $^3\Pi$	1774	1704	1697	1663	1725	9999	1679	1697
BH	A $^1\Pi$	2550	2480	2480	2473	2335	2309	2305	2251
	B $^1\Sigma^+$	2528	2498	2484	2476	2398	2390	2389	2400

Table 9: Adiabatic excitation energies T_e (eV) of diatomic molecules. For the technical details see Sec. 5.1; experimental values from Ref. [31].

Molecule	State	CIS	CIS(D)	ADC(2)	CC2	CCSD	CCSDR(3)	CC3	exp.
N_2	A $^3\Sigma_u^+$	5.30	6.70	6.62	6.54	6.33	-	6.13	6.22
	B $^3\Pi_g$	7.71	7.64	7.44	7.31	7.59	-	7.38	7.39
	B′ $^3\Sigma_u^-$	7.52	8.79	8.70	8.67	8.62	-	8.19	8.22
	a′ $^1\Sigma_u^-$	7.52	8.82	8.73	8.72	8.82	8.54	8.43	8.45
	a $^1\Pi_g$	9.60	8.86	8.56	8.39	8.85	8.67	8.61	8.59
	w $^1\Delta_u$	8.13	9.46	9.36	9.37	9.34	9.04	8.90	8.94
	C $^3\Pi_u$	11.82	11.51	11.29	11.24	11.23	-	11.11	11.05
CO	a $^3\Pi$	5.78	6.26	6.18	6.08	6.17	-	6.02	6.04
	A $^1\Pi$	8.82	8.24	8.07	7.97	8.26	8.11	8.04	8.07
	B $^1\Sigma^+$	12.02	11.49	11.35	11.11	11.21	10.96	10.94	10.78
	C $^1\Sigma^+$	12.57	11.79	11.88	11.64	11.75	11.51	11.50	11.40
BF	a $^3\Pi$	2.73	3.44	3.42	3.43	3.59	-	3.60	3.61
	A $^1\Pi$	6.56	6.39	6.37	6.36	6.40	6.34	6.34	6.34
	b $^3\Sigma^+$	7.24	7.73	7.67	7.57	7.69	-	7.57	7.57
	B $^1\Sigma^+$	8.33	8.35	8.33	8.22	8.29	8.16	8.15	8.10
	C $^1\Sigma^+$	8.51	8.74	8.72	8.64	8.71	8.62	8.63	8.56
	d $^3\Pi$	8.58	8.87	8.85	8.77	8.87	-	8.76	8.77
BH	A $^1\Pi$	2.85	2.79	2.80	2.80	2.90	2.86	2.88	2.87
	B $^1\Sigma^+$	6.41	6.54	6.48	6.48	6.57	6.52	6.54	6.49